Dalton
Transactions

Accepted Manuscript

This article can be cited before page numbers have been issued, to do this please use: D. Chao and M. Zhao, *Dalton Trans.*, 2019, DOI: 10.1039/C9DT00407F.

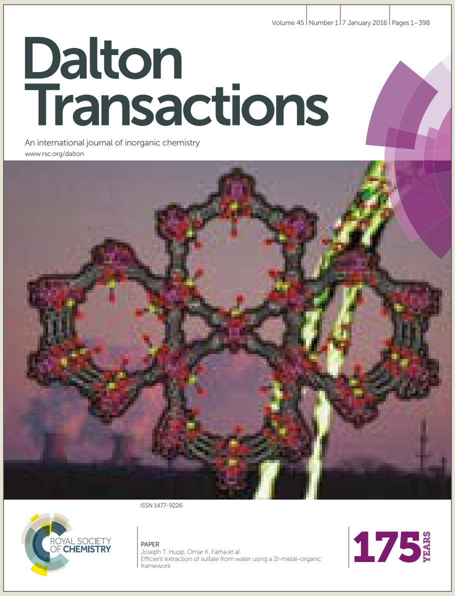

Volume 45 | Number 1 | 7 January 2016 | Pages 1–398

Dalton Transactions

An international journal of inorganic chemistry
www.rsc.org/dalton

ISSN 1477-9226

ROYAL SOCIETY OF CHEMISTRY

PAPER
Joseph T. Hupp, Omar K. Farha et al.
Efficient extraction of sulfate from water using a Zr-metal–organic framework

175 YEARS

ROYAL SOCIETY OF CHEMISTRY

rsc.li/dalton

View Article Online
DOI: 10.1039/C9DT00407F

Journal Name

ARTICLE

Received 00th January 20xx,
Accepted 00th January 20xx

DOI: 10.1039/x0xx00000x

www.rsc.org/

A supramolecular assembly bearing organic TADF chromophore: synthesis, characterization and light–driven cooperative acceptorless dehydrogenation of secondary amines

Duobin Chao*[a] and Mengying Zhao[b]

A noble–metal–free chromophore–catalyst supramolecular assembly, which is composed of organic thermally activated delayed fluorescence (TADF) chromophore and cobaloximes, has been designed and synthesized for the first time for efficient acceptorless dehydrogenation of secondary amines under blue light irradiation at room temperature. The TADF chromophore has a long lifetime of 17.4 μs with suitable redox potentials for selective acceptorless dehydrogenation of secondary amines to afford imines and H_2 through cooperative catalysis of the chromophore and cobaloximes in the supramolecular assembly. A high TON of 895 was obtained for acceptorless dehydrogenation of 1,2,3,4–tetrahydroisoquinoline despite its high oxidation potential (+ 1.38 V vs. SCE).

Introduction

Chromophore–catalyst supramolecular assemblies have been employed as considerable photocatalysts in many homogeneous and heterogeneous light–driven processes such as hydrogen evolution,[1] carbon dioxide reduction,[2] dye–sensitized photoelectrochemical cells (DSPEC)[3-5] and organic transformations[6, 7]. In general, light–absorbing chromophores are covalently linked to specific catalysts through a bridging ligand in supramolecular assemblies and then undergo cooperative catalysis with adjacent catalysts. The chromophores play vital roles in light harvesting and electron transfer processes, and they are commonly composed of transition meal complexes such as Ir^{III}[8] and Ru^{II}[9] complexes. These transition metal complexes have long excited–state lifetimes and tunable redox potentials that make them capable of promoting various photocatalytic reactions. However, ruthenium and iridium are rare and noble metals. Therefore, non–precious organic chromophores with long lifetimes are promising for constructing supramolecular assemblies. Although several organic chromophores such as BODIPY compounds[10] and fluorescein[11] have been employed to construct supramolecular photocatalysts, substrates with low oxidation potentials (e. x. TEA and TEOA) are required as well as limited turnover numbers (TONs). Moreover, halogenation (Br and I) is strongly required to achieve long–lived excited state to achieve efficient catalysis, resulting in more complicated synthetic routes and poorer photophysical properties. Donor–acceptor (D–A) organic chromophores show intramolecular charge transfer upon light irradiation and may have long lifetimes such as thermally activated delayed fluorescence (TADF) compounds with no need of halogenation,[12] which have been investigated in biosensing,[13] OLEDs,[14] solar cells[15] and photocatalytic reactions[16]. Moreover, synthetic routes of D–A type TADF chromophores are well investigated and their photophysical properties and redox potentials are tunable as noble metal complexes.[17] In this context, organic TADF chromophores may be good candidates to construct chromophore–catalyst supramolecular assemblies. Chromophore–catalyst supramolecular assemblies bearing such D–A type TADF chromophores for photocatalytic reactions have yet to be explored.

Catalytic acceptorless dehydrogenation (CAD) is an attractive strategy for hydrogen release from liquid organic hydrogen carriers (LOHCs) that are believed as potential materials for hydrogen storage due to reversible hydrogenation and dehydrogenation.[18-20] However, acceptorless dehydrogenation of LOHCs is rarely conducted under mild conditions due to high temperature.[21, 22] Secondary amines usually have low melting points and some secondary amines are liquid at room temperature, which makes secondary amines as potential nitrogen–containing LOHCs using reversible conversion between secondary amines and imines.[23] Highly efficient and selective acceptorless dehydrogenation of secondary amines along with H_2 release is poorly investigated in homogeneous catalysis. Most procedures for oxidative dehydrogenation of secondary amines in the presence of stoichiometric oxidants could not

---

[a] *School of Materials Science and Chemical Engineering, Ningbo University, Zhejiang 315211, China. Email: chaoduobin@nbu.edu.cn*
[b] *School of Petroleum and Chemical Engineering, Dalian University of Technology, Panjin, Liaoning 124221, China.*

†Electronic Supplementary Information (ESI) available: NMR spectra and HRMS spectra. See DOI: 10.1039/x0xx00000x

View Article Online
DOI: 10.1039/C9DT00407F

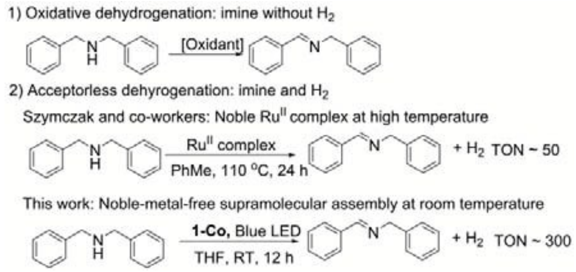

Scheme 1 Dehydrogenation of secondary benzylamine.

release H_2.[24, 25] Szymczak and co–workers reported solely selective acceptorless dehydrogenation of secondary amines to imines (e.x. secondary benzylamine) using a noble Ru^{II} catalyst at 110 °C after 24 h (Scheme 1).[26] Additionally, the turnover number (TON) of CAD reactions was relatively low (~50). It remains a challenge to achieve noble–metal–free acceptorless dehydrogenation of secondary amines with high TON and selectivity at room temperature. On the other hand, CAD of amines provides an alternative to obtain imines with high atom economy. As a proof of concept, we herein report the first supramolecular assembly which consists of D–A type TADF chromophore and Co^{III} moieties for CAD of secondary amines at room temperature under visible light irradiation.

Results and discussion

The assembly **1–Co**, which looks like an android (four Co^{III} complexes as the legs and arms and **1** as the body and head), has been prepared facilely as shown in Scheme 2. **1–Co** was first characterized by NMR and high–resolution electrospray ionization mass spectrometry (HR–ESI–MS). The m/z signal at 2538.4026 (calcd. 2538.4212) in the MS spectrum of **1–Co** is assigned to species $[M + Na]^+$ (M = **1–Co**) (Fig. S1), suggesting **1** was successfully tethered to four Co^{III} moieties. Additionally, isotopic signals are distributed with an interval of 1 in accordance with +1 charge of species $[M + Na]^+$ (Fig. S2). The cobaloxime $Co(dmgH)_2PyCl$ is a well–known hydrogen evolution catalyst that has been used with various photosensitizers.[27-29] Thus, we chose it to collaborate with **1** and examine performance of **1** in the supramolecular photocatalyst **1–Co**.

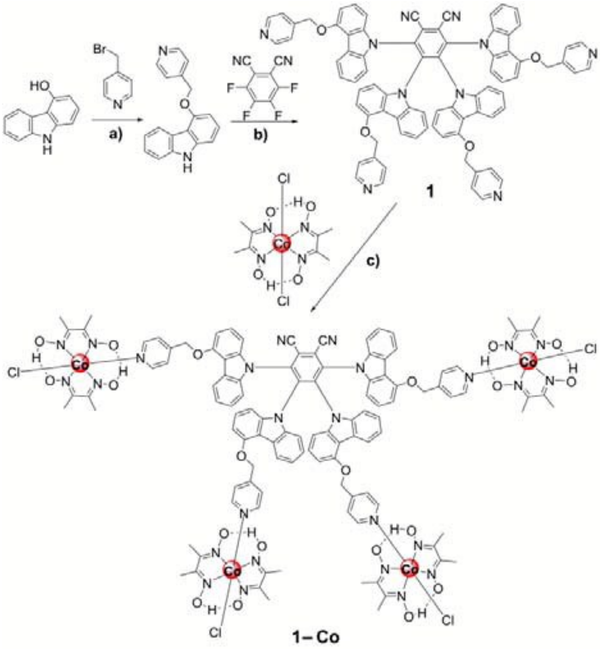

Scheme 2 Synthetic routes of chromophore **1** and assembly **1–Co**. a) K_2CO_3, DMF, 70 °C and 12 h; b) NaH, THF, 40 °C and 16 h; c) CH_2Cl_2/CH_3OH (v/v = 1:1), NEt_3, 12 h and room temperature.

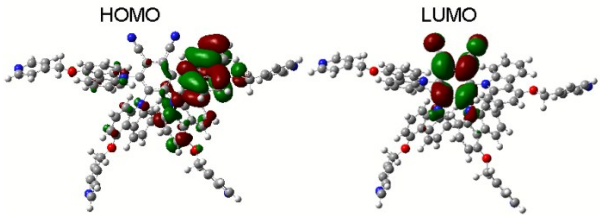

Fig. 1 HOMO and LUMO for chromophore **1** by DFT calculations.

We further found **1** could absorb moderate visible light (Fig. S3). Its emission was structureless and centered at 591 nm with a relative quantum yield of 7.2 % in dichloromethane using $[Ru(bpy)_3]^{2+}$ as the standard (Fig. S3). The broad emission showed blue shift in solvents with lower polarity such as THF and toluene (Fig. S4), suggesting intramolecular charge transfer of **1**. This solvatochromic effect can be ascribed to the D–A nature of **1**. The density functional theory (DFT) calculation was then carried out to confirm the D–A structure (Fig. 1 and S5). The highest occupied molecular orbital (HOMO) of **1** is mainly delocalized over the electron–rich carbazolyl groups as the donor (D) and the lowest unoccupied molecular orbital (LUMO) of **1** is mainly distributed on the electron–deficient benzonitrile groups as the acceptor (A). Moreover, similar DFT results were observed when one Co^{III} moiety was tethered to **1** (Fig. S6). A charge transfer (CT) state from carbazolyl groups to benzonitrile groups can be expected upon light irradiation.

The HOMO and LUMO are highly isolated and ΔE_{ST} of **1** was found to be 0.13 eV, which are characteristic nature for D–A type TADF compounds.[17] It is known that long–lived charge transfer state is important for transition metal complexes to mediate electron transfer processes in photocatalytic reactions. We then found the photoluminescence lifetime of **1** was 17.4 μs in degassed dichloromethane at room temperature (Fig. S7), which was comparable to lifetimes of polypyridine ruthenium(II) complexes such as popular $[Ru(bpy)_3]^{2+}$ (0.87 μs). Such a long lifetime ensures sufficient time for **1** to promote photocatalytic reactions. These results demonstrate chromophore **1** possesses appropriate photophysical properties as an efficient photosensitizer in photoredox catalysis under visible light irradiation.

Redox potentials of **1** including electrochemical properties of ground state and excited state were further studied to confirm thermodynamic feasibility of electron transfer between **1** and $Co(dmgH)_2PyCl$. The cyclic voltammetry (CV) programs of **1** showed the oxidation potential $E(\mathbf{1}^+/\mathbf{1})$ ($\mathbf{1}^+$ =

View Article Online
DOI: 10.1039/C9DT00407F

oxidized **1**) was + 1.39 V vs. SCE (Fig. S8). According to the ground–state oxidation potential and zero–zero excitation energy ($E_{0,\,0}$ = 2.10 eV) that was calculated from the emission of **1** at 591 nm, the excited–state oxidation potential $E(\mathbf{1}^+/\mathbf{1}^*)$ was determined as – 0.71 V vs. SCE ($E(\mathbf{1}^+/\mathbf{1}^*) = E(\mathbf{1}^+/\mathbf{1}) - E_{0,\,0}$).[30] Thus, the oxidative quenching of excited state of **1** (**1***) by Co(dmgH)$_2$PyCl (E(Co^{III}/Co^{II}) = – 0.67 V vs. SCE) is thermodynamically available (ΔG = – 0.04 eV). The fluorescence titration experiments further verified that **1*** can be oxidatively quenched by Co(dmgH)$_2$PyCl (Fig. S9).

The assembly **1–Co** displayed weaker emission than chromophore **1** with a quantum yield of 2.9% and the absorption spectrum is similar to **1** (Fig. S10). The quenching of emission was probably due to electron transfer from **1** to Co^{III}. Energy transfer between **1** and Co^{III} is negligible because the emission of **1** lies beyond absorption of Co^{III}. The emission lifetime of **1–Co** decreases a little bit by comparison with **1** and was determined to be 13.8 μs (Fig. S11), indicating Co^{III} has slight influence on the photophysical properties of **1**. Nevertheless, redox potentials of separated **1** and Co(dmgH)$_2$PyCl were observed in the CV spectrum of assembly **1–Co** (Fig. S12). For instance, the irreversible redox waves at – 0.63 V and + 1.38 V vs. SCE are assigned to Co^{III}/Co^{II} and **1**$^+$/**1**, respectively. The reduction potentials of **1** and Co^{II}/Co^{I} are approximate and overlapped around –1.12 V vs. SCE.[8] These results suggest two components **1** and Co(dmgH)$_2$PyCl have no significant electronic interaction at ground state in the supramolecular assembly **1–Co**.

Encouraged by feasible electron transfer between **1*** and Co(dmgH)$_2$PyCl, we next employed assembly **1–Co**, **1** and Co(dmgH)$_2$PyCl (abbreviated as Co^{III}) in photocatalytic CAD of secondary amines. Initially, secondary benzylamine **2a** was used as the substrate to examine generation of imine and H$_2$ in dry THF. Dry THF was used here to ensure **2a** as the only hydrogen source of H$_2$. As shown in Fig. 2, efficient H$_2$ release was observed in degassed dry THF solution containing **1–Co** and **2a** upon light irradiation with blue LEDs at room temperature. A TON of 305 was obtained after 12 h of irradiation (Table 1, entry 1). However, **1–Co** displayed much lower TON when CH3CN was used as the solvent, which is probably due to ligand disassociation in CH$_3$CN that has been studied by Eisenberg and co–workers. A lower TON of 53 was observed for the multicomponent system including separated **1** and Co(dmgH)$_2$PyCl (Table 1, entry 5). The higher TON for supramolecular photocatalytic system is probably due to more feasible electron transfer from **1*** to Co(dmgH)$_2$PyCl when they are linked through covalent bond. Additionally, emission of **1** is barely quenched by **2a** according to titration experiment (Fig. S13). Then we can conclude that the catalytic cycle begins with oxidative quenching of **1*** by Co(dmgH)$_2$PyCl. That is to say, covalent linkage is positively helpful for oxidative quenching of **1*** by Co(dmgH)$_2$PyCl, resulting in higher efficiency when assembly **1–Co** was used. We further found imine **3a** was generated by ^{1}H NMR, indicating successful acceptorless dehydrogenation of **2a** with H$_2$ release. Control experiments showed that visible light and two components were all required to achieve efficient acceptorless dehydrogenation, indicating the catalytic cycle is light–driven cooperative catalysis process. We examined performance of [Ru(bpy)$_3$]$^{2+}$ for CAD of **2a**. However, unlike CAD of 2–MeTHQ (THQ = tetrahydroquinoline) with [Ru(bpy)$_3$]$^{2+31}$, no detectable H$_2$ was found (Table 1, entry 8). This is probably due to high oxidation potential of **2a** (E_{Ox}(**2a**$^{+\bullet}$/**2a**) = + 1.37 V vs. SCE) (Fig. S15), which is higher than Ru(bpy)$_3^{2+}$ (E(Ru$^{III/II}$) = + 1.29 V vs. SCE).

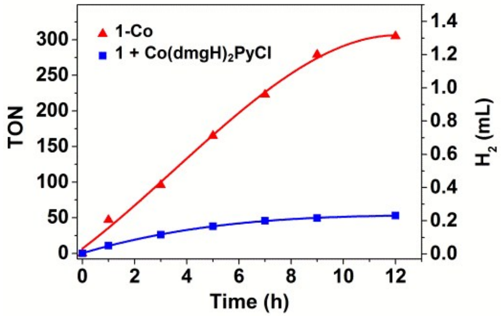

Fig. 2 Time–dependent H$_2$ release from **2a** (0.5 mmol) with assembly **1–Co** (0.2 μmol) and separated system containing **1** (0.2 μmol) and Co(dmgH)$_2$PyCl (0.8 μmol) in THF (8 mL) at room temperature under blue light irradiation.

Table 1 Photocatalytic acceptorless dehydrogenation of **2a**.[a]

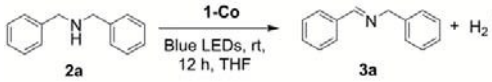

Entry	Variation from the standard conditions	TON (H$_2$)[b]
1	none	305
2	no visible light	0
3	no THF, CH$_3$CN as the solvent	60
4	no **1–Co**	0
5[c]	no **1–Co**, adding **1** and Co^{III}	53
6	no **1–Co**, adding Co^{III}	0
7	no **1–Co**, adding **1**	0
8[d]	no **1–Co**, adding [Ru(bpy)$_3$]$^{2+}$ and Co^{III}	0

[a] Standard conditions: **2a** (0.5 mmol), **1–Co** (0.2 μmol) and THF (8 mL) under blue light irradiation for 12 h at room temperature. [b] TON = n(H$_2$)/n(chromophore). [c] **1** (0.2 μmol) and Co^{III} (0.8 μmol). [d] [Ru(bpy)$_3$]$^{2+}$ (0.2 μmol) and Co^{III} (0.8 μmol).

It is worth mentioning that light–driven CAD of secondary amine **2a** for H$_2$ release is significantly different from H$_2$ evolution from water using tertiary amines such as TEA (E_{Ox}(TEA) = + 0.69 V *vs.* SCE) as substrate, because tertiary amines have much lower oxidation potentials than **2a**. When tertiary amines were used, photosensitizers (e. x. Ir^{III} complexes) are commonly reductively quenched by TEA. Additionally, tertiary amines are decomposed along with generation of complicated by–products that could not undergo reversible dehydrogenation–hydrogenation process.[32]

Acceptorless dehydrogenation of other secondary amines including **2b**, **2c** and **2d** was also investigated (Table 2). A higher TON of 360 was obtained for the substrate with low

View Article Online
DOI: 10.1039/C9DT00407F

Table 2 Photocatalytic acceptorless dehydrogenation of various secondary amines.[a]

Entry	Substrate	Product	Sel. (%)	TON (H_2)[b]
1	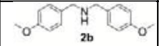 2b	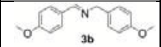 3b	99	360
2	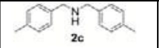 2c	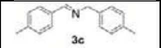 3c	99	301
3	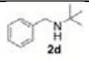 2d	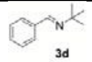 3d	99	50
4	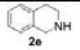 2e	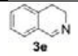 3e	96	895
5[c]	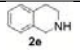 2e	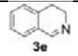 3e	96	538
6[d]	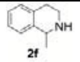 2f	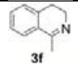 3f	98	604

[a]Standard conditions: substrate (0.5 mmol), **1–Co** (0.2 µmol) and THF (8 mL) under blue light irradiation for 12 h at room temperature. [b]TON = n(H_2)/n(**1–Co**). [c]**1–Co** (0.4 µmol), **2e** (0.25 mmol). [d]**2f** (0.25 mmol), **1–Co** (0.4 µmol).

oxidation potential such as **2b** (E_{Ox}(**2b**$^{+\bullet}$/**2b**) = + 1.25 V vs. SCE)(Fig. S16), while **2d** (E_{Ox}(**2d**$^{+\bullet}$/**2d**) = + 1.49 V vs. SCE) (Fig. S18) with high oxidation potential showed poor TON of 50. Nevertheless, **2a** release one H_2 (~1.0 wt%). We then tested **1–Co** in the photocatalytic CAD of another kind of secondary amines such as N–heterocyclic compound **2e**. **2e** also released one H_2 but with 1.5 wt%. Additionally, **3e** was generated with a TON of 895 when the amount of **1–Co** was 0.2 µmol (Table 2, entry 4). The apparent quantum yield (AQY) at 450 nm was estimated to be 2.1% when **1–Co** was 0.4 µmol and the yield of **3e** was 86%. **2f** was dehydrogenated to **3f** in 96% yield (TON = 604) when more **1–Co** was used (Table 2, entry 6). The yield was calculated with isolated **3f** after careful column chromatography. Although released hydrogen content of these amines and yields of imines are still relatively low, these results are helpful for developing noble–metal–free photocatalytic acceptorless dehydrogenation of secondary amines as well as other nitrogen–containing LOHCs.

To know better about the catalytic cycle, we monitored changes of UV–vis absorption spectra of **1–Co** in the presence of **2a** upon light irradiation. As can be seen from Fig. 3, at t = 0 min, no obvious absorption peak was observed from 400 to 500 nm. After the solution was irradiated for 4 min, the absorption increased and a shoulder peak appeared in the range of 400 to 500 nm. The enhancement was ascribed to formation of Co^{II} species, indicating an electron transfer from **1*** to Co^{III} along with generation of Co^{II}.[27] We also observed slight enhancement of absorption in the range of 550 to 700 nm, which can be assigned to Co^{I} species.[27]

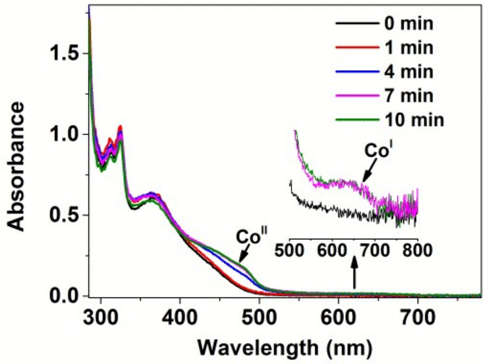

Fig. 3 Time–dependent absorption spectra of **1** (25 µM) in the presence of **2a** (50 mM) in degassed dry THF (3 mL) upon blue light irradiation at room temperature.

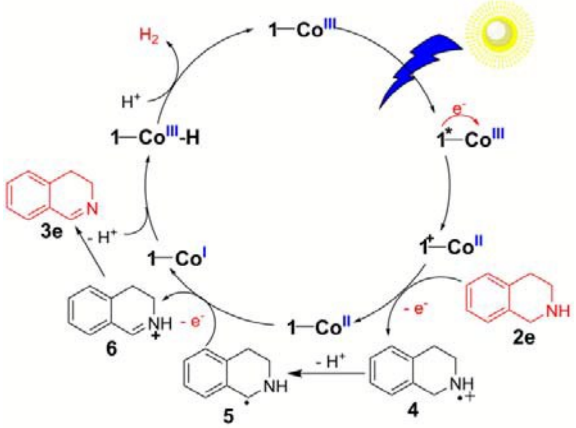

Fig. 4 Plausible mechanism for CAD of **2e** using **1–Co**.

On the basis of the above results, we proposed a plausible mechanism for hydrogen release from **2e** (Fig. 4). Initially, **1–Co^{III}** achieves the excited state **1*–Co** under blue light irradiation along with subsequent electron transfer from **1*** to Co^{III}. The resulting **1^{+}** then oxidize **2e** to generate radical cation **4**.[33] The deprotonation of **4** would produce strongly reducing radical **5** that is further oxidized to iminium ion **6** by Co^{II}. Deprotonation of **6** affords dehydrogenation product **3e**.[34] Meanwhile, Co^{II} is reduced to Co^{I}. It is worth noting that Co^{II} could not be reduced by excited state 1*, because higher potential of E(**1^{+}**/**1***) (–0.71 V) than E(Co^{II}/Co^{I}) (–1.12 V). Further protonation of Co^{I} leads to Co^{III}–H. Co^{III}–H is then protonated to release H_2 along with generation of Co^{III} for next catalytic cycle. Other pathway such as homolysis of Co^{III}–H to generate H_2 and Co^{II} is not ruled out.[28]

Conclusions

In summary, we developed a unique supramolecular assembly for highly efficient CAD of secondary amines under blue light irradiation at room temperature. The supramolecular assembly is composed of an organic TADF chromophore as light–harvesting unit and Co^{III} complexes as catalytic center. An electron transfer from the chromophore to Co^{III} center occurs upon light irradiation and they further undergo cooperative catalysis for enhaced acceptorless dehydrogenation of secondary amines. Secondary amines were selectively converted to corresponding imines despite their high oxidation potentials. The highest TON of 895 was achieved. Our results show a promising noble–metal–free strategy for CAD reactions through cooperative photocatalysis. Organic D–A type TADF chromophores are developed increasingly, which indicates

DOI: 10.1039/C9DT00407F

that more efficient CAD of secondary amines may be established by using more suitable. We expect organic TADF chromophores will be applied in light–driven acceptorless dehydrogenation of more organic substrates at room temperature.

Conflicts of interest

There are no conflicts to declare.

Experimental section

Materials and instruments

All starting materials were purchased from commercial suppliers and used as received. Dry THF (water < 50 ppm) was used. Co(dmgH)(dmgH$_2$)Cl$_2$[35] and Co(dmgH)$_2$PyCl[35] were synthesized as reported. ^{1}H NMR spectra were carried out using a Bruker Avance 500 MHz instrument with tetramethysilane (TMS) as an internal standard. HRMS (ESI) spectra were recorded using a Thermofisher Q–Exactive instrument. Emission spectra were measured by Lengguang Tech. Instruments (F97PRO) with Xe lamp as the light source. UV–vis absorption spectra were obtained on a PerkinElmer Lambda 950 spectrophotometer. Cyclic voltammetry (CV) was carried out on CHI660E in a one–compartment cell equipped with a glassy carbon working electrode, a saturated calomel electrode reference electrode, and a platinum plate counter electrode at a scan rate of 0.1 V s^{-1} at room temperature. The potentials were referenced to SCE through an internal standard oxidation of ferrocene. GC analysis was carried out on Scion 436/456 (TCD detector, N$_2$ carrier gas, 5 Å molecular sieve column). Transient PL spectrum was carried out with Edinburgh Instruments FLS980 Spectrometer at room temperature. Incident photons were measured on a solar power meter from Shenzhen Sanpo Instrument Co., Ltd.

Synthesis and characterization

4–(pyridin–4–ylmethoxy)–9H–carbazole. 9H–carbazol–4–ol (180 mg, 1 mmol) and 4–(bromomethyl)pyridine (171 mg, 1 mmol) were dissolved in DMF (15 mL). Then K$_2$CO$_3$ (270 mg, 2 mmol) was added into the solution. The mixture was stirred at 70 °C for 12 h. Then DMF was removed under reduced pressure. The resulting precipitate was dissolved in water and filtered to collect filter cake. The filter cake was further purified to obtain brown solid by silica gel column chromatography (CH$_2$Cl$_2$/CH$_3$OH = 100:1). Yield: 40%. ^{1}H NMR (500 MHz, DMSO–d$_6$), δ (ppm): 11.33 (s, 1H), 8.64 (d, 2H, J = 5.0 Hz), 8.19 (d, 1H, J = 5.0 Hz), 7.57 (d, 2H, J = 5.5 Hz), 7.47 (d, 1H, J = 8.0 Hz), 7.36 (t, 1H, J = 7.5 Hz), 7.30 (t, 1H, J = 8.0 Hz), 7.17 (t, 1H, J =7.5 Hz), 7.11 (d, 1H, J = 8.0 Hz), 6.76 (d, 1H, J = 8.0 Hz), 5.45 (s, 2H). ^{13}C NMR (125 MHz, DMSO–d$_6$), δ (ppm): 154.57, 150.34, 146.97, 141.70, 139.49, 126.91, 125.21, 122.62, 122.25, 122.00, 119.29, 112.02, 111.04, 104.91, 101.46, 68.41. HR–ESI–MS (m/z): found 275.1215 for [*M* + H]$^+$ (calcd. 275.1179, C$_{18}$H$_{15}$N$_2$O$^+$).

Chromophore 1. 4–(pyridin–4–ylmethoxy)–9H–carbazole (230 mg, 0.84 mmol) was dissolved in THF (20 mL). NaH (35 mg, 1.4 mmol) was added and stirred for 30 min at room temperature under N$_2$ atmosphere. Then 3,4,5,6–tetrafluorophthalonitrile (42 mg, 0.21 mmol) was added into the solution. The mixture was further stirred at 40 °C for 16 h under N$_2$ atmoshpere. After the solution was cooled to room temperature, water was added to quench excess NaH. Then THF was removed under reduced pressure and water was added to the residue. The aqueous solution was extracted with CH$_2$Cl$_2$ three times. The organic layer was collected and CH$_2$Cl$_2$ was further removed under rotary evaporator to give brown powder. The brown powder was then purified to give yellow powder by silica gel column chromatography (CH$_2$Cl$_2$/CH$_3$OH = 50:1). Yield: 85%. ^{1}H NMR (500 MHz, DMSO–d$_6$), δ (ppm): 8.60 (t, 4H, J = 6.5 Hz), 8.46–8.50 (m, 4H), 7.92–7.95 (m, 2H), 7.70–7.76 (m, 2H), 7.37–7.50 (m, 10H), 7.07–7.22 (m, 12H), 6.74–6.82 (m, 4H), 6.54–6.64 (m, 4H), 6.38 (t, 2H, J = 7.5 Hz), 5.31–5.33 (m, 4H), 5.07 (t, 4H, J = 10.0 Hz). ^{13}C NMR (125 MHz, DMSO–d$_6$), δ (ppm): 154.01, 153.20, 150.31, 150.08, 146.48, 146.32, 142.25, 141.79, 140.90, 140.84, 139.69, 138.81, 138.75, 138.68, 137.56, 126.85, 125.64, 124.91, 123.88, 122.65, 122.29, 121.91, 121.34, 119.96, 113.75, 112.60, 112.34, 111.42, 105.20, 104.33, 103.87, 68.26, 67.84. HR–ESI–MS (m/z): found 1217.4146 for [*M* + H]$^+$ (calcd. 1217.4246, C$_{80}$H$_{53}$N$_{10}$O$_4^+$).

Assembly 1–Co. Co(dmgH)(dmgH$_2$)Cl$_2$ (36 mg, 0.1 mmol) was added to a reaction flask and then CH$_3$OH (15 mL) was added to afford a suspension. NEt$_3$ (20 µL) was added to the suspension and stirred for 30 min to form a brown solution. A solution of 1 (27 mg, 0.022 mmol) in CH$_2$Cl$_2$ was added slowly through a dropping funnel. The mixed solution was stirred for 6 h at room temperature under air atmosphere. CH$_3$OH was added to afford yellow precipitate. The precipitate was collected through filtration and washed with CH$_3$OH to afford 1–Co after drying under vacuo. Yield: 92%. ^{1}H NMR (500 MHz, DMSO–d$_6$), δ (ppm): 8.58–8.61 (m, 1H), 8.45–8.49 (m, 1H), 8.07 (s, 3H), 7.97 (s, 3H), 7.88–7.97 (m, 2H), 7.68–7.73 (m, 2H), 7.54–7.63 (m, 4H), 7.37–7.45 (m, 6H), 7.25–7.30 (m, 4H), 7.04–7.20 (m, 8H), 6.71–6.81 (m, 4H), 6.50–6.63 (m, 4H), 6.35–6.38 (m, 2H), 5.33–5.37 (m, 4H), 5.10–5.16 (m, 4H), 2.31–2.34 (m, 24H), 2.26–2.28 (m, 24H). ^{13}C NMR (125 MHz, DMSO–d$_6$), δ (ppm): 153.69, 153.64, 153.01, 152.72, 151.17, 151.05, 150.61, 150.40, 142.04, 141.67, 140.79, 139.56, 137.40, 124.08, 123.88, 123.85, 123.80, 113.67, 112.47, 111.39, 111.33, 111.23, 105.47, 105.40, 67.32, 66.86, 13.15, 13.09. HR–ESI–MS (m/z): found 2538.4026 for [*M* + H]$^+$ (calcd. 2538.4212, C$_{112}$H$_{108}$Cl$_4$Co$_4$N$_{26}$NaO$_{20}^+$).

General procedure for photocatalytic H$_2$ release

The THF solution (8 mL) containing catalyst (1–Co, 1 and Co^{III}) and substrates was added to a tube equipped with a small stir bar. Then the tube was degassed by N$_2$ and then irradiated with 16 blue LEDs (450 ± 10 nm, 3W) at room temperature. The reaction was monitored through H$_2$ generation. H$_2$ was determined by GC. The headspace was analyzed by periodically sampling 100 µL with a sample lock syringe. When

View Article Online
DOI: 10.1039/C9DT00407F

H_2 increased no more, the reaction was stopped and solvent was removed in vacuum. Then crude products were collected and further purified by column chromatography over silica for 3e and 3f using CH_2Cl_2/CH_3OH (neutral alumina for 2a, 2b, 2c and 2d using hexane/CH_2Cl_2). TONs were determined by n(H_2)/n(1–Co) or n(H_2)/n(1) for the reaction of entry 4 in Table 1.

Acknowledgements

This work has been supported by National Natural Science Foundation of China (No. 21605013) and K. C. Wong Magna Fund in Ningbo University.

Notes and references

1. M. G. Pfeffer, B. Schafer, G. Smolentsev, J. Uhlig, E. Nazarenko, J. Guthmuller, C. Kuhnt, M. Wachtler, B. Dietzek, V. Sundstrom and S. Rau, *Angew. Chem. Int. Ed.*, 2015, **54**, 5044-5048.
2. R. Kuriki, M. Yamamoto, K. Higuchi, Y. Yamamoto, M. Akatsuka, D. Lu, S. Yagi, T. Yoshida, O. Ishitani and K. Maeda, *Angew. Chem. Int. Ed.*, 2017, **56**, 4867-4871.
3. N. Kaeffer, J. Massin, C. Lebrun, O. Renault, M. Chavarot-Kerlidou and V. Artero, *J. Am. Chem. Soc.*, 2016, **138**, 12308-12311.
4. D. L. Ashford, M. K. Gish, A. K. Vannucci, M. K. Brennaman, J. L. Templeton, J. M. Papanikolas and T. J. Meyer, *Chem. Rev.*, 2015, **115**, 13006-13049.
5. M. S. Eberhart, K.-R. Wee, S. Marquard, K. Skinner, D. Wang, A. Nayak and T. J. Meyer, *ChemSusChem*, 2017, **10**, 2380-2384.
6. D. Chao and M. Zhao, *ChemSusChem*, 2017, **10**, 3358-3362;
7. W. Iali, P.-H. Lanoe, S. Torelli, D. Jouvenot, F. Loiseau, C. Lebrun, O. Hamelin and S. Ménage, *Angew. Chem. Int. Ed.*, 2015, **54**, 8415-8419.
8. C. Lentz, O. Schott, T. Auvray, G. Hanan and B. Elias, *Inorg. Chem.*, 2017, **56**, 10875-10881.
9. G. F. Manbeck, E. Fujita and K. J. Brewer, *J. Am. Chem. Soc.*, 2017, **139**, 7843-7854.
10. G. G. Luo, K. Fang, J. H. Wu and J. Mo, *Chem. Commun.,* 2015, **51**, 12361-12364.
11. T. M. McCormick, Z. Han, D. J. Weinberg, W. W. Brennessel, P. L. Holland and R. Eisenberg, *Inorg. Chem.*, 2011, **50**, 10660-10666.
12. Y. Im, M. Kim, Y. J. Cho, J.-A. Seo, K. S. Yook and J. Y. Lee, *Chem. Mater.*, 2017, **29**, 1946-1963.
13. D. Chao, S. Ni and W. Mu, *Chem. Lett.*, 2016, **45**, 27-29.
14. H. Uoyama, K. Goushi, K. Shizu, H. Nomura and C. Adachi, *Nature*, 2012, **492**, 234-238.
15. J.-S. Wu, S.-W. Cheng, Y.-J. Cheng and C.-S. Hsu, *Chem. Soc. Rev.*, 2015, **44**, 1113-1154.
16. J. Luo and J. Zhang, *ACS Catalysis*, 2016, **6**, 873-877.
17. Z. Yang, Z. Mao, Z. Xie, Y. Zhang, S. Liu, J. Zhao, J. Xu, Z. Chi and M. P. Aldred, *Chem. Soc. Rev.*, 2017, **46**, 915-1016.
18. P. Preuster, C. Papp and P. Wasserscheid, *Acc. Chem. Res.*, 2017, **50**, 74-85.
19. J. G. West, D. Huang and E. J. Sorensen, *Nat. Commun.*, 2015, **6**, 10093.
20. S. Kato, Y. Saga, M. Kojima, H. Fuse, S. Matsunaga, A. Fukatsu, M. Kondo, S. Masaoka and M. Kanai, *J. Am. Chem. Soc.*, 2017, **139**, 2204-2207.
21. M. Kojima and M. Kanai, *Angew. Chem. Int. Ed.*, 2016, **55**, 12224-12227.
22. K. I. Fujita, T. Wada and T. Shiraishi, *Angew. Chem. Int. Ed.*, 2017, **56**, 10886-10889.
23. R. H. Crabtree, *ACS Sustainable Chem. Eng.*, 2017, **5**, 4491-4498.
24. G. Jiang, J. Chen, J.-S. Huang and C.-M. Che, *Org. Lett.*, 2009, **11**, 4568-4571.
25. R. Kumar, E. H. Gleißner, E. G. V. Tiu and Y. Yamakoshi, *Org. Lett.*, 2016, **18**, 184-187.
26. K.-N. T. Tseng, A. M. Rizzi and N. K. Szymczak, *J. Am. Chem. Soc.*, 2013, **135**, 16352-16355.
27. P. Du, K. Knowles and R. Eisenberg, *J. Am. Chem. Soc.*, 2008, **130**, 12576-12577.
28. T. M. McCormick, B. D. Calitree, A. Orchard, N. D. Kraut, F. V. Bright, M. R. Detty and R. Eisenberg, *J. Am. Chem. Soc.*, 2010, **132**, 15480-15483.
29. G. Zhang, C. Liu, H. Yi, Q. Meng, C. Bian, H. Chen, J.-X. Jian, L.-Z. Wu and A. Lei, *J. Am. Chem. Soc.*, 2015, **137**, 9273-9280.
30. Y. Zhang, J. L. Petersen and C. Milsmann, *J. Am. Chem. Soc.*, 2016, **138**, 13115-13118.
31. K. H. He, F. F. Tan, C. Z. Zhou, G. J. Zhou, X. L. Yang and Y. Li, *Angew. Chem. Int. Ed.,* 2017, **56**, 3080-3084.
32. Y. Pellegrin and F. Odobel, *C. R. Chim.*, 2017, **20**, 283-295.
33. J. Hu, J. Wang, T. H. Nguyen and N. Zheng, *Beilstein J. Org. Chem.*, 2013, **9**, 1977-2001.
34. D. B. Ushakov , M. B. Plutschack , K. Gilmore and P. H. Seeberger , *Chem. Eur. J.*, 2015, **21**, 6528-6534.
35. W. C. Trogler, R. C. Stewart, L. A. Epps and L. G. Marzilli, *Inorg. Chem.*, 1974, **13**, 1564-1570.